

IMPACT MODEL RESOLUTION ON PAINLEVÉ'S PARADOX*

ZHAO Zhen (赵 振)[†] CHEN Bin (陈 滨) LIU Caishan (刘才山) JIN Hai (金 海)

(Department of Mechanics and Engineering Science, Peking University, Beijing 100871, China)

ABSTRACT: Painlevé's paradox is one of the basic difficulties for solving LCP of dynamic systems subjected to unilateral constraints. A bi-nonlinear parameterized impact model, consistent with dynamic principles and experimental results, is established on the localized and quasi-static impact model theory. Numerical simulations are carried out on the dynamic motion of Painlevé's example. The results confirm "impact without collision" in the inconsistent states of the system. A "critical normal force" which brings an important effect on the future movement of the system in the indeterminate states is found. After the motion pattern for the impact process is obtained from numerical results, a rule of the velocity's jump that incorporates the tangential impact process is deduced by using an approximate impulse theory and the coefficient of restitution defined by Stronge. The results of the jump rule are quite precise if the system rigidity is big enough.

KEY WORDS: Painlevé's paradox, inconsistent, indeterminate, impact without collision, tangential impact

1 INTRODUCTION

Dynamical systems with unilateral constraints have attracted much attention due to their relevance in high-tech, especially in aerospace technology^[1]. Although very complicated structures are involved in practice^[2], the theoretical difficulties of the unilateral constraint systems can be found in very simple configurations and Painlevé's example is acknowledged as one.

Painlevé's example is shown in Fig.1. There is an isotropic slender rod with one end A sliding on the ground. The length of the rod is $2l$, the mass is m and the angle between the rod and ground is θ . The contact point A is subjected to Coulomb's friction law (with friction coefficient being μ). F_n and F_t are normal and tangential contact forces, respectively.

According to Ref.[3] the relationship between the normal acceleration \ddot{y}_A and the normal force F_n on the contact point can be expressed as

$$\ddot{y}_A = A(\theta, \mu)F_n + B(\theta, \dot{\theta}) \quad (1)$$

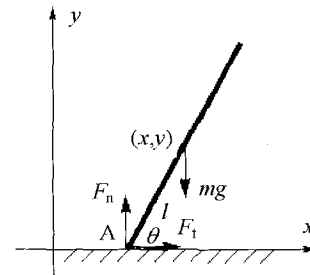


Fig.1 Painlevé's example

with

$$A(\theta, \mu) = \frac{1}{m}(1 + 3 \cos \theta (\cos \theta - \mu \sin \theta)) \quad (2)$$

and

$$B(\theta, \dot{\theta}) = l\dot{\theta}^2 \sin \theta - g \quad (3)$$

It is proven^[3] that if $\mu > 4/3$, there are four cases of LCP (Linear Complementarity Problem) as depicted in Fig.2 by selecting proper values of θ and $\dot{\theta}$ on the basis of (1):

Received 27 June 2003, revised 2 March 2004

* The project supported by the National Natural Science Foundation of China (10272002), Doctoral Foundation of Educational Ministry of China (20020001032) and the foundation (02413200203235)

[†] E-mail: ssyyt@sina.com

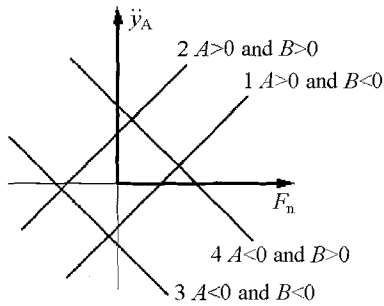


Fig.2 Relationship between F_n and \ddot{y}_A

Case 1: $A > 0, B < 0$. This situation corresponds to continual sliding leftwards, which is given by the solution $\dot{y}_A = 0, F_n > 0$.

Case 2: $A > 0, B > 0$. The rod leaves the surface due to inertia and the solution is $\ddot{y}_A > 0, F_n = 0$.

Case 3: $A < 0, B < 0$. There is no solution at all and it is inconsistent.

Case 4: $A < 0, B > 0$. It is clear that continual sliding and separation are possible solutions for the rod. It is indeterminate.

Painlevé gave a method called LCP to solve such unilateral constraint systems as one in Fig.1. When the rod moves into the indeterminate or inconsistent states, LCP can not be solved. Due to this fact, Painlevé' paradox is known. It is an acknowledged method to solve LCP of dynamical systems subjected to unilateral constraints^[2] and this method is supported by a number of algorithms^[4]. However, Painlevé' paradox is one of the basic difficulties to the algorithms.

Many scientists have studied the problem since Painlevé brought forward Painlevé' paradox. The possibility of solutions with velocity discontinuities to the inconsistent case was first recognized by Lecornu, or perhaps more or less at the same time by Bolotov^[3]. The velocity jump of Painlevé' example in the inconsistent state means that the comparative normal speed \dot{y}_A is zero at the moment. So it is called "impact without collision (IW/OC)" for such impact or "tangential impact". Now a question arises: How can we compute the velocity jump? Baraff^[3] proposed the following rules:

(1) Since the inconsistency is caused by dynamic friction, the impulse must convert at least one of the contact points to static friction.

(2) The contact impulse must be such that the bodies do not separate after the discontinuity.

Baraff's rules provide a jump rule for the velocities after a tangential impact occurs. But one may argue whether it is true for a real jump. Yu Wang^[5]

provided another jump rule using Routh's diagram method in terms of a proper collision model and he believed that the jump process should be divided into two phases: In the first phase, the rod moves along the line of limiting friction; In the second phase, it moves along the line of sticking.

Some questions may be asked:

(1) Is it true that "impact without collision" will occur when dynamical systems are in the inconsistent state?

(2) If it is true, what is the jump rule?

(3) How to obtain interactive forces and motion in detail when the impact occurs including IW/OC if the actual unilateral constraints of the dynamical systems are not absolutely rigid?

Song^[6] provided an effective method to study Painlevé's paradox. He used a compliant contact model with the parameter of local rigidity tending to infinite to simulate the impact process. The contact model he used is a continuous viscoelastic damp impact one and the plastic effect is not considered by him. His research concerns only with the case of indeterminate state.

A bi-nonlinear impact model, in which the plastic distortion is the only form of energy dissipation, is established on the basis of local and quasi-static impact model theory^[7] in this paper. The impact model is also based on contact mechanics and results of experiments. Coulomb's dry friction is considered in the tangential direction neglecting compliance. We have carried out numerical researches on all the cases of dynamic motion of Painlevé's example using normal and tangential models. (We call this method the softened method.) The effects of different dynamic motions starting from general initial states as well as initial states with surface energy of unilateral constraints are considered here. The instances of dynamic motions of the system in actual cases by using the softened method as well as cases when the system converges to a rigid-body one are studied.

Our research indicates that the numerical results converge to the unique solution $\ddot{y}_A = 0, F_n > 0$ of LCP in Case 1 of Painlevé' example as the elastic modulus tends to infinity. The inertial-jump-up solution by using the softened impact model agrees with the unique jump-up solution of LCP in Case 2 when no initial surface energy exists.

The softened solutions converge to "IW/OC" in Case 3 when no initial surface energy exists. The jump rule depends on the normal and tangential impact models. For the impact models we use, the

jump rule is made up of three phases: tangential impact phase while the tangential speed at the contact point changes from negative to zero at the end of this phase; sticking-compression phase; sticking-restitution phase. In the last part of this paper, the jump rule is given in detail on the basis of an approximate impulse theory. The numerical research indicates that the theoretical results of the jump rule are quite accurate if the system rigidity is big enough.

The dynamic motion has complicated structure in Case 4 as the initial surface energy is an important factor which affects the future motion form of the system. The inertial-jump-up solution of LCP in Case 4 is the only possible one if the initial surface energy is zero. Although another sliding solution ($F_n^* = -B/A$) of LCP in Case 4 is also a theoretical one, it is not a stable one. The dynamic motion will depart far from it once disturbance exists. The dynamic motion forms of the system are not consistent with each other entirely with the change of the initial normal force at the contact point. The dynamic motion forms are divided into two groups in the indeterminate states of Painlevé's example. In the first group, the initial normal force at the contact point is less than F_n^* and the dynamic motion is close to the inertial-jump-up solution of LCP in Case 4. In the second group, the initial normal force is greater than F_n^* and the dynamic motion is just like IW/OC.

The impact models we use agree with the actual material contact and impact rule. The numerical results obtained not only give proper answers to Painlevé's paradox, but contain detailed information of forces and motion during the impact process of the dynamical systems subject to unilateral constraints. The information obtained is very useful in practical design.

2 PARAMETERIZED IMPACT MODEL AND SURFACE ENERGY

The impact models used not only are convenient to the research work of Painlevé's paradox, but also agree with the material impact law. The process of impact is very complicated and the inconsistent contact area is small. So the localization is a very effective method for the impact process, in which the resultant force and moment are acquired instead of the actual impact process. Because the speeds of stress wave are much greater than the relative impact speeds in a low speed impact, it is reasonable to assume that the stresses due to an impact are transmitted to every particle in the body instantaneously, which is called

quasi-static method^[7].

The normal impact model is independent of the tangential motion in the condition of a low speed impact. The tangential model neglects compliance and is only subjected to Coulomb's friction law. There are many normal force-displacement impact models: linear spring-damping models, nonlinear spring-damping models and bi-nonlinear spring-damping models. For these impact models, we will consider bi-nonlinear spring-damping models. Because impact forces are very great and the duration of impact is relatively short, the plastic distortion is local. Johnson^[8] applied Hertz theory and the von Mises yield criterion to determine the normal force at which the incipient yield occurs in two spheres subjected to a normal load. Loc Vu-Quoc and Xiang Zhang^[9] proposed a normal force-displacement model for contact spheres accounting for plastic deformation based on finite element theory. A relationship between the normal force and normal displacement is established through the formalism of the continuum mechanics of elasto-plasticity by Liu Caishan^[10] and the contact yield stress definition clearly accounts for the plastic deformation. Shivaswamy^[11] presented a bi-nonlinear impact model in his Doctoral thesis using modified Hertzian contact theory. He revised the exponent of relative displacement and gave a relationship between plastic permanent deformation and coefficient of restitution on the basis of experimental results. Because the last impact model agrees with the experimental results, we modify and use it in this paper.

2.1 Impact Model in Compressional Phase

In the compressional phase of impact, the relationship between normal force and relative displacement can be written as

$$F_n = K_e \delta^n \quad (4)$$

where n is the modified constant exponent. K_e is stiffness and δ is normal deformation. In Hertzian theory

$$n = 3/2 \quad K_e = 4/3E^*R^{*1/2}$$

with

$$\frac{1}{R^*} = \frac{1}{R_1'} + \frac{1}{R_1''} + \frac{1}{R_2'} + \frac{1}{R_2''}$$

$$\frac{1}{E^*} = \frac{1 - \nu_1^2}{E_1} + \frac{1 - \nu_2^2}{E_2}$$

where R_1' and R_1'' are two principal curvature radii at the contact point of one body and R_2' and R_2'' two

principal curvature radii of another body. E_i is material elastic modulus and ν_i is Poisson's ratio.

The force-displacement model in restitution phases is given by

$$F_n = F_{n \max} \left(\frac{\delta - \delta_p}{\delta_{\max} - \delta_p} \right)^n \quad (5)$$

where δ_{\max} and $F_{n \max}$ represent the maximum deformation and the maximum normal force. We modify Shivaswamy's suggestion here and obtain δ_{\max} and $F_{n \max}$ at the exact time when $\dot{\delta} = 0$ and $\ddot{\delta} < 0$ at the end of the compressional phase with impact process being continuous.

The parameter δ_p in (5) represents the permanent deformation during the impact and depends not only on the energetic coefficient of restitution e_s , but on the maximum deformation δ_{\max}

$$\delta_p = \delta_{\max}(1 - e_s^2) \quad (6)$$

Here the plastic distortion is the only form of the energy dissipation that is assumed. In terms of (4), the work the normal force F_n does during the compressional phase of impact can be expressed as

$$W_c = \int_0^{\delta_{\max}} F_n d\delta = K_e \frac{\delta_{\max}^{n+1}}{n+1} = \frac{F_{n \max} \delta_{\max}}{n+1} \quad (7)$$

In terms of (5), the work the normal force F_n does during the restitution phase of impact can be written by

$$W_r = \int_{\delta_{\max}}^{\delta_p} F_n d\delta = -\frac{F_{n \max}(\delta_{\max} - \delta_p)}{n+1} \quad (8)$$

Here Stronge's energetic coefficient of restitution e_s is properly considered as

$$W_r = -e_s^2 W_c \quad (9)$$

By substituting W_c and W_r from (7) and (8), δ_p becomes the form of (6).

2.2 Surface Energy in Unilateral Constraints

For the dynamical systems subjected to unilateral constraints we must distinguish the softened method in which the system converges to a rigid-body one and LCP in which the system is a rigid-body. When the softened method is used, the dimensions with the unilateral constraints are free and the free dimensions appended contain the initial "surface energy". But in the rigid systems with unilateral constraints the energy reserved can not be considered at all due to the dimensions constrained. The initial "surface energy" must be expressed in other way, the

initial normal force at the contact area for example, since it has a critical effect on the future movement of the systems.

Integrate (4) from zero to the initial deformation δ_0 in the contact area

$$E_{n0} = \frac{K_e \delta_0^{n+1}}{n+1} = \frac{F_{n0} \delta_0}{n+1} \quad (10)$$

where E_{n0} is considered as the initial surface energy and F_{n0} is the initial normal contact force.

3 NUMERICAL RESEARCH ON DYNAMICS FOR PAINLEVÉ'S EXAMPLE USING SOFTENED IMPACT MODEL

In order to make the problem clear, the values of parameters of Painlevé's example are $m = 1 \text{ kg}$, $l = 1 \text{ m}$, $g = 9.8 \text{ kg} \cdot \text{m/s}^2$ and the static and kinetic frictional coefficient is supposed to be $\mu = 1.4$. The rod moves as a rigid body as a whole in the softened method and the impact models are introduced and applied locally at the contact area. The rod and the ground are assumed to be of the same material. The value of exponent is $n = 1.764$ according to the experimental result in Ref.[11]. The elastic modulus is $E = 20.9 \times 10^{10} \text{ N/m}^2$, which can be changed in the numerical research. The Poisson's ratio $\nu = 0.3$ and the radius of contact end A $R = 0.00645 \text{ m}$. The energetic coefficient of restitution is assumed to be a constant $e_s = 0.75$.

In the numerical research the system of Painlevé's example is considered, which is made up of three kinetic forms: sliding, sticking and free flying without contacting the ground. The transform conditions must be given properly. When the contact point A of the rod is sliding on the ground, $|F_t| = \mu F_n$. When point A of rod is sticking on the ground, $\dot{x}_A = 0$ and $\ddot{x}_A = 0$ if the sticking is holding. By using dynamic equations and the condition $\ddot{x}_A = 0$, the tangential force F_t at the contact area can be expressed as

$$F_t = \frac{3 \sin \theta \cos \theta F_n - m l \dot{\theta}^2 \cos \theta}{3 \sin^2 \theta + 1}$$

The condition on which sticking holds is $|F_t| \leq \mu F_n$. When the rod is free without contacting the ground, $F_n = F_t = 0 \text{ N}$.

Additionally it is assumed that there is only one kinetic form in one step during computing process as sliding, sticking or free flying. It is reasonable if the length of step is very small and the numerical results obtained will be precise enough.

3.1 Unique Solution of LCP for $A > 0, B < 0$

The initial state of Painlevé's example is shown in Table 1.

Table 1 Initial state (unit: IU)

x_A	\dot{x}_A	y_A	\dot{y}_A	θ	$\dot{\theta}$	A	B
0	-1	0	0	0.5	1.0	1.5434	-9.3206

Linear complementary solution in Painlevé is shown in Fig.3. Obviously, the unique solution is the rod sliding leftwards on the ground and the normal contact force $F_n = -B/A = 6.039\text{ N}$.

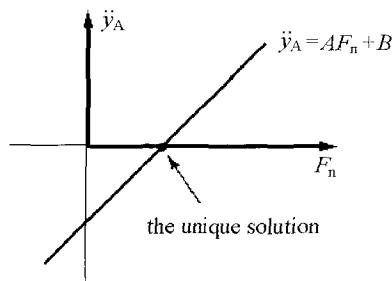
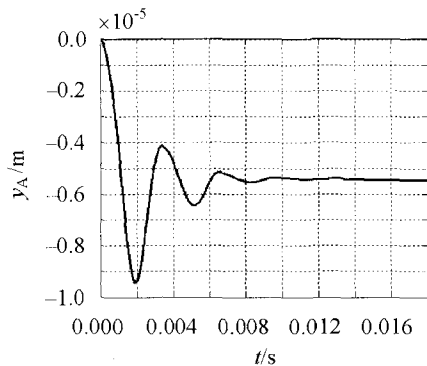


Fig.3 Unique solution of LCP for $A > 0, B < 0$

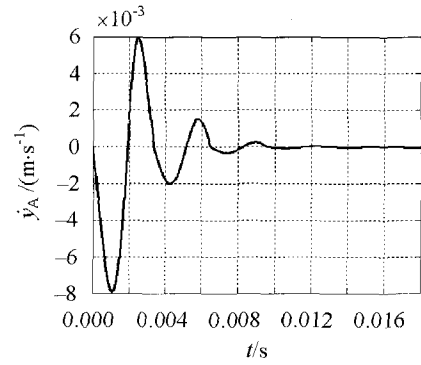
In the softened method, the initial state is the same as the one in Table 1. The numerical results are shown in Fig.4 ($E = 20.9 \times 10^{10}\text{ N/m}^2$).

Starting from the initial state, the normal displacement y_A (Fig.4(a)) and normal force F_n (Fig.4(c)) at the contact point stop oscillating and become stable at 6.40 N after a period of time (0.01 s) when the normal speed \dot{y}_A turns to zero and holds.

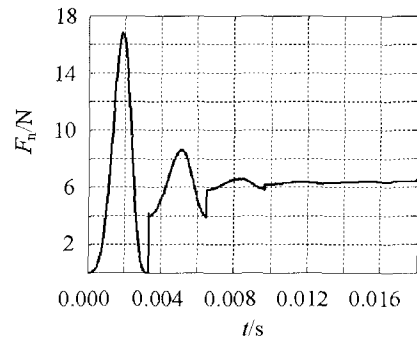
If we increase elastic modulus to $E = 20.9 \times 10^{14}\text{ N/m}^2$, from the initial state the normal force F_n oscillates for about $0.75 \times 10^{-3}\text{ s}$ and then becomes stable at 6.071 N (Fig.4(d)) as compared with the value $-B/A = 6.039\text{ N}$.



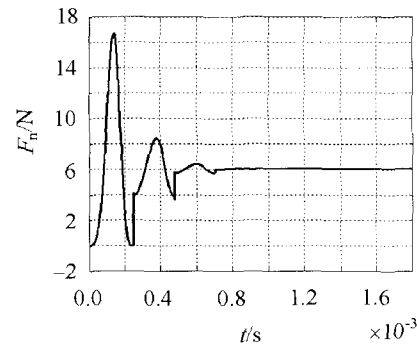
(a) History of y_A



(b) History of \dot{y}_A



(c) History of F_n for $E = 20.9 \times 10^{10}\text{ N/m}^2$



(d) History of F_n for $E = 20.9 \times 10^{14}\text{ N/m}^2$

Fig.4 Numerical results for $A > 0, B < 0$

All the numerical results above show that the bigger the elastic modulus is, the less time period of the system undergoes from starting to stable state with no obvious impact appearing. In addition, the results also reveal that starting from initial state with small initial surface energy, the dynamic characters and motion trend to remain unchanged.

When $A > 0$ and $B < 0$ and the system converges to a rigid-body, the solution $F_n = -B/A, \dot{y}_A = 0$ of LCP in Painlevé's example is just appropriate.

3.2 Unique Solution of LCP for $A > 0, B > 0$

The solution of LCP is shown in Fig.5 and the normal acceleration \ddot{y}_A is positive, which means that the rod will jump up from ground. So the normal force F_n and tangential force F_t are zeroes. We call this solution of LCP the inertial-jump-up solution. We can test the rationality of the solution straight away.

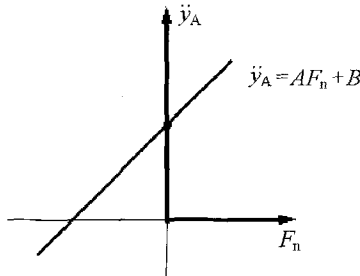


Fig.5 Unique solution in LCP for $A > 0, B > 0$

If we remove the contact plane in Fig.1, the dynamical equations can be written as

$$\begin{aligned} m\ddot{x} &= 0 \\ m\ddot{y} &= -mg \\ J\ddot{\theta} &= 0 \end{aligned} \tag{11}$$

where normal acceleration \ddot{y}_A at the contact point is

$$\ddot{y}_A = \ddot{y} - l\ddot{\theta} \cos \theta + l\dot{\theta}^2 \sin \theta \tag{12}$$

Substitute \ddot{y} and $\ddot{\theta}$ from (11) to (12), we have

$$\ddot{y}_A = -g + l\dot{\theta}^2 \sin \theta \tag{13}$$

If $B > 0$, by (13) we know that $\ddot{y}_A > 0$. So the rod would jump directly if there was no unilateral constraint. If there is a unilateral constraint and the rod slips on the ground ($F_n \geq 0$), the normal acceleration and normal force should satisfy the relationship $\ddot{y}_A = AF_n + B$. Therefore when $A > 0$ and $B > 0$, $\ddot{y}_A > 0$ and the rod will always jump up inertially.

The initial state used by the softened method is shown in Table 2 with elastic modulus $E = 20.9 \times 10^{10} \text{ N/m}^2$. From Fig.6, one can find that the rod jumps up inertially and obviously no interaction forces exist in the contact area. The numerical results are consistent with the solution of LCP when $A > 0$ and $B > 0$.

Table 2 Initial state (unit: IU)

x_A	\dot{x}_A	y_A	\dot{y}_A	θ	$\dot{\theta}$	A	B
0	-1	0	0	0.5	5	1.5434	2.1856

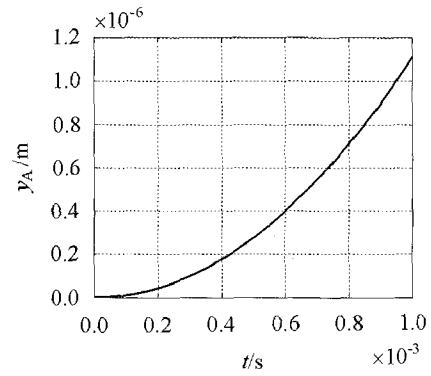


Fig.6 History of y_A for $A > 0, B > 0$

3.3 Inconsistent State of Painlevé's Example ($A < 0, B < 0$)

The frictional coefficient is $\mu = 1.4 > 4/3$ in all examples of this paper. The system of Painlevé's example is just in the inconsistent state when $A < 0, B < 0$ if the initial state is selected as shown in Table 3. The solution of LCP is shown in Fig.7 and obviously there is no solution at all.

Table 3 Initial state (unit: IU)

x_A	\dot{x}_A	y_A	\dot{y}_A	θ	$\dot{\theta}$	A	B
0	-1	0	0	1.0	1.0	-0.0037	-8.9585

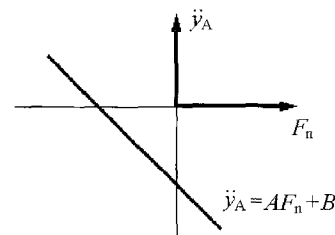
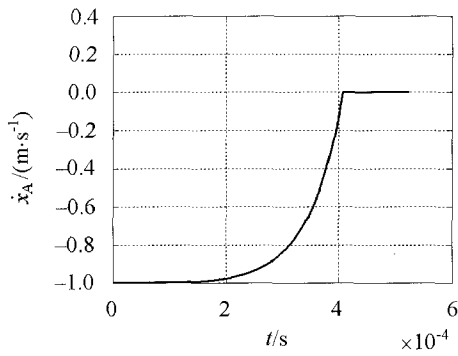


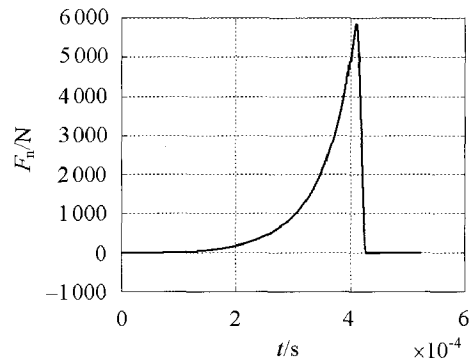
Fig.7 No solution in Painlevé's paradox

Elastic modulus used by the softened method is bigger than the one before (here $E = 20.9 \times 10^{14} \text{ N/m}^2$) to get a smaller response period of time. The numerical results are shown in Fig.8.

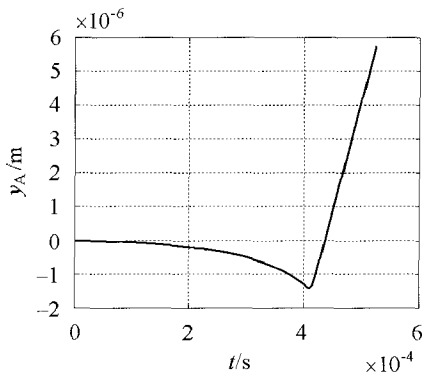
In Fig.8 the tangential speed \dot{x}_A at the contact point turns from sliding leftwards to sticking in a very short time (about $4 \times 10^{-4} \text{ s}$ in (a) of Fig.8), which is the result of "tangential impact" produced by great frictional force F_t . At the same time of Tangential Impact, there is a deformation in the contact area ((b) of Fig.8), which results in a downward velocity at the contact point ((c) of Fig.8) and the rotational speed $\dot{\theta}$ jumps to increase ((d) of Fig.8). In view of energy, by the tangential impact, a portion of the leftwards-



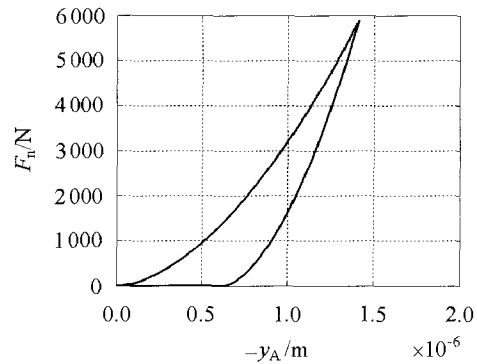
(a) History of \dot{x}_A



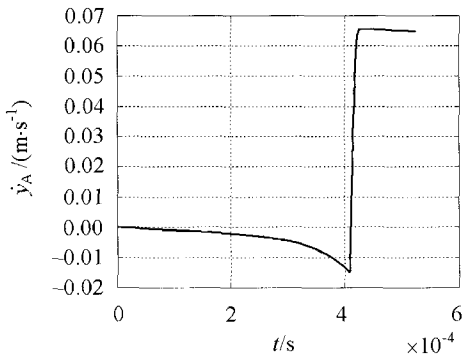
(e) History of F_n



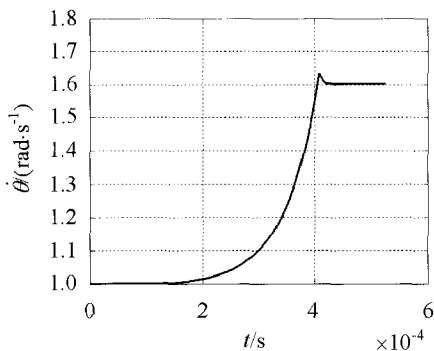
(b) History of y_A



(f) F_n changing with $(-y_A)$



(c) History of \dot{y}_A



(d) History of $\dot{\theta}$

Fig.8 Numerical results of Painlevé's example in the inconsistent state

sliding kinetic energy of the rod is transformed into the compressional potential energy, a portion into the downwards-moving kinetic energy and a portion into the rotational kinetic energy. Just after the tangential impact, the system continues in the compressional phase while the contact point is sticking on the ground for a shorter period of time (about 10^{-4} s). In this period the compressional potential energy and rotational energy of the rod continue to increase. At the end of the second period, the normal speed \dot{y}_A becomes zero when the compressional phase ends and the restitution phase begins. During the restitution phase (the third period), the rod keeps sticking on the ground until it bounces up by resilience and the rotational speed $\dot{\theta}$ falls down a little ((d) of Fig.8). Now the whole process of impact is achieved.

The maximum normal contact force ((e) of Fig.8) and permanent deformation ((f) of Fig.8) in the contact area can be also found in Fig.8, which may help to see the special behavior of the impact process above.

By using the softened method, more comprehensive dynamic properties of Painlevé's example can be

found.

The process above is getting closer to an “impact” with the increase of elastic modulus (Fig.9). The whole impact process involves a very short period of time comparing with the period (about 2.3 s) of the same single pendulum in gravity. It is in this short time that the general velocities as \dot{x}_A , \dot{y}_A and $\dot{\theta}$ change rapidly and only “velocity jump” can describe such phenomena, which is just the characteristic of “impact without collision”. “Negative inertia” maybe appears by the coupling interactions between normal force and tangential force when the frictional coefficient is big enough in dynamic systems subjected to unilateral constraints. Once negative inertia appears, pressure in one direction may lead to acceleration in the opposite direction. This “regenerative feedback” will result in impact. It is called the frictional “catastrophe”^[12] in literature. Tangential sticking can help the system to escape from it.

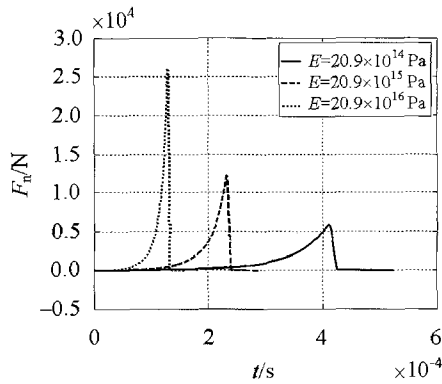


Fig.9 History of F_n

Different initial speeds \dot{x}_A in the tangential direction do not affect the impact time greatly by fixing elastic modulus as shown in Fig.10. The system with the shortest impact time in Fig.10 possesses the initial surface energy and others do not. The dynamic

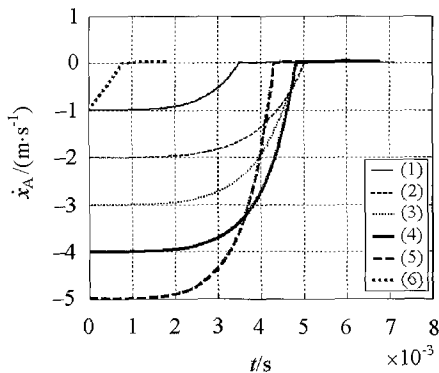


Fig.10 History of \dot{x}_A from different initial states

process is different from that described above if the initial value of $\dot{\theta}$ is in the inconsistent field and near the border by fixing elastic modulus. The value of $\dot{\theta}$ will escape from the inconsistent field during the dynamic process. However, with the increase of elastic modulus, such phenomena will rarely occur.

3.4 Indeterminate State of Painlevé’s Example
($A < 0, B > 0$)

In Painlevé’s example, two solutions appear as $A < 0$ and $B > 0$ if $\mu > 4/3$, which is another difficulty of LCP. In this instance we select the initial state of the system listed in Table 4. The two solutions of LCP are shown in Fig.11. One of the solutions is $F_n = 0, \ddot{y}_A > 0$, which is called the inertial-jump-up solution. Another solution is $F_n > 0, \ddot{y}_A = 0$, which is called the sliding-leftward solution and satisfies the relationship $F_n = -B/A$.

Table 4 Initial state (unit: IU)

x_A	\dot{x}_A	y_A	\dot{y}_A	θ	$\dot{\theta}$	A	B
0	-1	0	0	1	5	-0.0337	11.2368

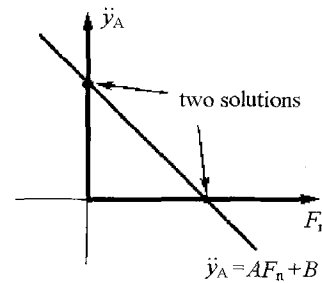


Fig.11 Two solutions of Painlevé’s example

First, three initial states are considered as listed in Table 5 ($E = 20.9 \times 10^{14} \text{ N/m}^2$), where the state (1) is the general one in which no initial surface energy exists and other two initial states are the disturbance of state (1). The initial normal forces are 150 N and 300 N, respectively, in state (2) and state (3).

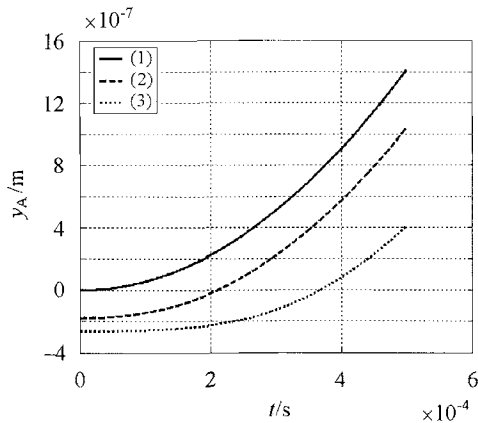
Table 5 Initial states (unit: IU)

	(1)	(2)	(3)
x_A	0	0	0
\dot{x}_A	-1	-1	-1
y_A	0	-1.7628×10^{-7}	-2.6113×10^{-7}
\dot{y}_A	0	0	0
θ	1	1	1
$\dot{\theta}$	5	5	5
A	-0.0337	-0.0337	-0.0337
B	11.2368	11.2368	11.2368

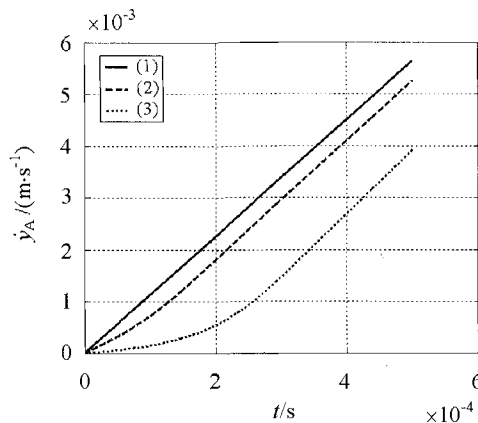
The numerical results are shown in Fig.12. Starting from the states listed in Table 5, the rod jumps up inertially ((a) and (b) in Fig.12) and the normal force F_n decreases to zero directly and rapidly ((d) in Fig.12), where the dynamic motion starting from initial state (1) is the inertial-jump-up solution of LCP when $A < 0$ and $B > 0$. No impact occurs at all ((d) in Fig.12).

Although another sliding solution ($F_n^* = -B/A$) of LCP is a theoretical one, it is not a stable one. If the initial normal force F_{n0} is less than F_n^* , the rod will jump up inertially (like Case 3 above). If $F_{n0} > F_n^*$, the system will move in the "negative inertia" field, which will lead to frictional "catastrophe", where the dynamic motion is just like IW/OC in inconsistent states.

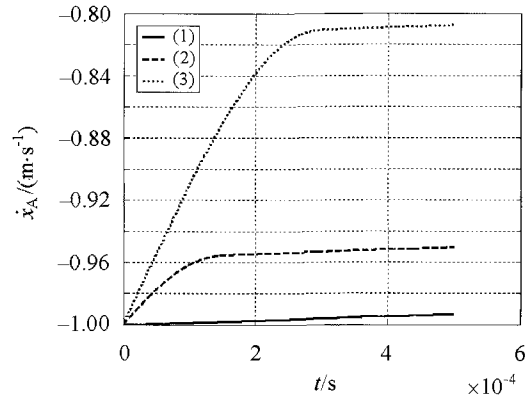
Another three initial states are considered (Table 6) here, which represent three kinds of states with bigger initial surface energy. The corresponding initial normal forces are 350 N, 500 N and 1 000 N ($E = 20.9 \times 10^{16} \text{ N/m}^2$). The numerical results are



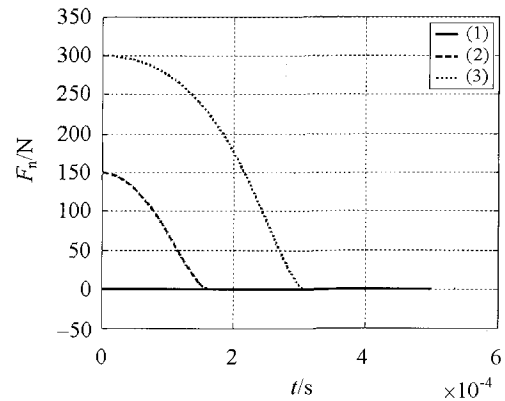
(a) History of y_A



(b) History of \dot{y}_A



(c) History of \dot{x}_A



(d) History of F_n

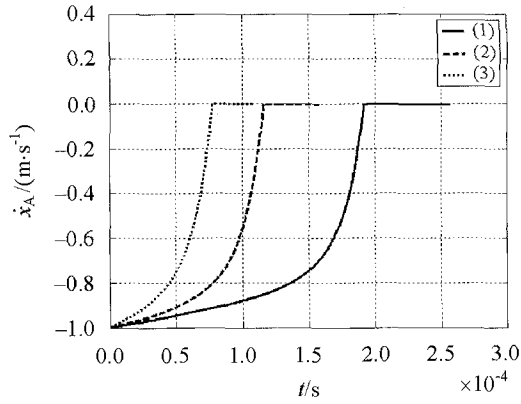
Fig.12 Numerical inertial-jump-up results of Painlevé's example in indeterminate states

shown in Fig.13. It is observed that starting from the states listed in Table 6, the dynamic motion is just like the one in the inconsistent field of the system.

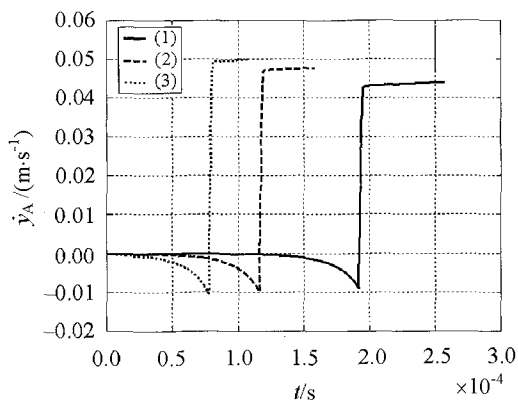
It is indicated in Fig.14 that the bigger the elastic modulus of the impact model is, the shorter time the impact will take and the bigger peak values the normal force will reach.

Table 6 Initial states (unit: IU)

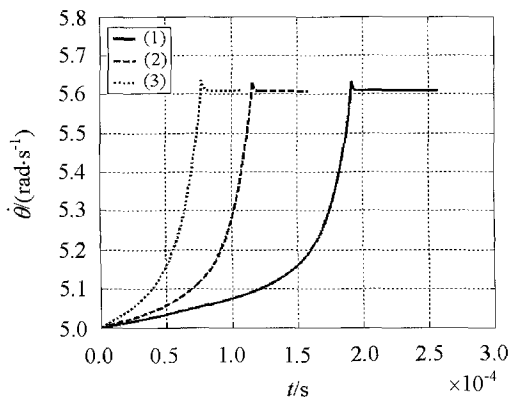
	(1)	(2)	(3)
x_A	0	0	0
\dot{x}_A	-1	-1	-1
y_A	-2.0942×10^{-8}	-2.5635×10^{-8}	-3.7974×10^{-8}
\dot{y}_A	0	0	0
θ	1	1	1
$\dot{\theta}$	5	5	5
A	-0.0337	-0.0337	-0.0337
B	11.2368	11.2368	11.2368



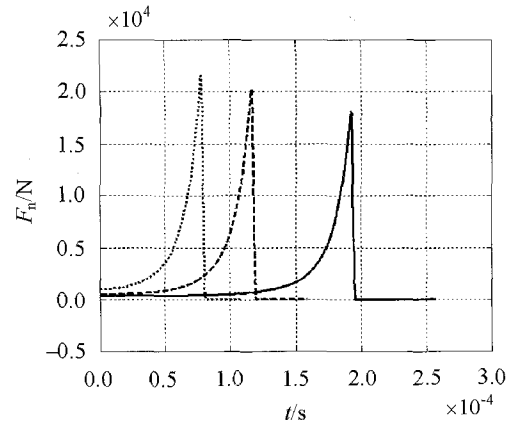
(a) History of \dot{x}_A



(b) History of \dot{y}_A



(c) History of $\dot{\theta}$



(d) History of F_n

Fig.13 Numerical impact results of Painlevé's example in indeterminate states

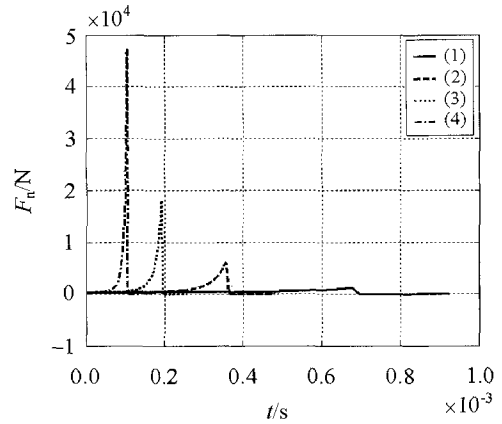


Fig.14 History of F_n in different conditions of elastic modulus

4 JUMP RULE

The numerical research shows how to overcome the difficulties in Painlevé's example. The conclusions are summarized as follows when no initial surface energy exists in the system:

- (1) If the system has a unique solution of LCP, there is no problem.
- (2) If the system has two solutions of LCP, the inertial-jump-up solution is selected.
- (3) If the system is in the inconsistent state, the "impact without collision" does happen.

The jump rule of IW/OC depends on the normal and tangential impact models. For the impact models we used, the jump rule is made up of three phases: tangential impact phase while the tangential speed at the contact point changes from negative to zero

at the end of this phase; sticking-compression phase; sticking-restitution phase. The velocities jump rules of the three phases can be obtained on the basis of an approximate impulse theory and the whole jump rule is made up of the three integrant rules.

4.1 Tangential Impact Phase $[t_0, t_1]$

If it is assumed that the rod slides leftwards, namely $\dot{x}_A(t_0) < 0$, the following conditions will be satisfied in this phase:

(1) The system is on the boundary of the cone of dry friction: $F_t = \mu F_n$.

(2) The tangential speed at the contact point changes from negative to zero at the end of this phase

$$\dot{x}(t) < 0 \quad t \in [t_0, t_1] \quad \text{and} \quad \dot{x}_A(t_1) = 0$$

Since $[t_0, t_1]$ is a very short period of time, the following assumptions are reasonable (the approximate impulse theory).

(1) The configuration of the system does not change during the time period $[t_0, t_1]$.

(2) Impulses of general forces including gravity and centrifugal forces are neglected during this period.

Integrating dynamic equations^[3] of Painlevé's example from t_0 to t_1 in terms of the assumptions above, we will obtain

$$\begin{aligned} \dot{x}_A(t_1) &= 0 \\ \dot{y}_A(t_1) &= \dot{y}_A(t_0) - \\ &\frac{1 - 3\mu \sin \theta \cos \theta + 3 \cos^2 \theta}{\mu - 3 \sin \theta \cos \theta + 3\mu \sin^2 \theta} \dot{x}_A(t_0) \end{aligned} \quad (14)$$

$$\dot{\theta}(t_1) = \dot{\theta}(t_0) - \frac{3\dot{x}_A(t_0)(\mu \sin \theta - \cos \theta)}{3l \sin \theta (\mu \sin \theta - \cos \theta) + \mu l}$$

$$P_{n1} = -\frac{m}{\mu - 3 \sin \theta \cos \theta + 3\mu \sin^2 \theta} \dot{x}_A(t_0)$$

For the need of the subsequent steps, the compressional potential energy accumulated need to be obtained. Since the rod is sliding leftwards in this period, then $F_t = \mu F_n$. So in this phase

$$\ddot{y}_A = A(\theta, \mu)F_n + B(\theta, \dot{\theta}) \quad (15)$$

Multiply (15) by \dot{y}_A and then by dt

$$d\left(\frac{\dot{y}_A^2}{2}\right) = A(\theta, \mu)F_n dy_A + B(\theta, \dot{\theta})dy_A$$

One is justified in writing

$$\frac{\dot{y}_A^2(t_1) - \dot{y}_A^2(t_0)}{2} = \int_{(t_0)}^{(t_1)} A(\theta, \mu)F_n dy_A +$$

$$\int_{(t_0)}^{(t_1)} B(\theta, \dot{\theta})dy_A \quad (16)$$

where F_n is the force that the ground acts on the end of the rod. So the force F'_n which the end of the rod acts on the ground is equal to $(-F_n)$ on the basis of Newton's Law. One obtains

$$\frac{\dot{y}_A^2(t_1) - \dot{y}_A^2(t_0)}{2} = - \int_{(t_0)}^{(t_1)} A(\theta, \mu)F'_n dy_A +$$

$$\int_{(t_0)}^{(t_1)} B(\theta, \dot{\theta})dy_A$$

Here the assumptions above are also suitable. Then $A(\theta, \mu)$ can be regarded as a constant. Parameter $\dot{\theta}$ is bounded and $B(\theta, \dot{\theta})$ is bounded too. So that $\int_{(t_0)}^{(t_1)} B(\theta, \dot{\theta})dy_A$ can be neglected.

$$En_1 = \int_{(t_0)}^{(t_1)} F'_n dy_A = -\frac{\dot{y}_A^2(t_1)}{2A(\theta, \mu)} \quad (17)$$

where En_1 is the compressional potential energy accumulated in the ground in the first phase.

4.2 Sticking-compression Phase $[t_1, t_2]$

There are two special features in this phase:

(1) The contact point of the rod is sticking on the ground in the tangential direction: $|F_t| \leq \mu F_n$ and $\dot{x}_A(t) = 0$, $t \in [t_1, t_2]$.

(2) The normal speed of the contact point of the rod turns from negative to zero: $\dot{y}_A(t) < 0$, $t \in [t_1, t_2]$ and $\dot{y}_A(t_2) = 0$.

Then by the approximate impulse theory, one can obtain

$$\dot{x}_A(t_2) = 0$$

$$\dot{y}_A(t_2) = 0$$

$$\dot{\theta}(t_2) = \dot{\theta}(t_1) + \frac{3 \cos \theta}{4l} \dot{y}_A(t_1) \quad (18)$$

$$P_{n2} = -m \frac{1 + 3 \sin^2 \theta}{4} \dot{y}_A(t_1)$$

Here the compressional potential energy is also needed in the subsequent steps. Since the rod is sticking on the ground in this phase, one is justified in writing

$$\ddot{y}_A = A'(\theta)F_n + B'(\theta, \dot{\theta}) \quad (19)$$

where

$$A'(\theta) = \frac{1}{m} \left(\frac{4}{1 + 3 \sin^2 \theta} \right)$$

$$B'(\theta, \dot{\theta}) = \frac{4l \sin \theta}{3 \sin^2 \theta + 1} \dot{\theta}^2 - g$$

Just using the same method in obtaining En_1 , one has

$$En_2 = -\frac{\dot{y}_A^2(t_2) - \dot{y}_A^2(t_1)}{2A'(\theta)} = \frac{\dot{y}_A^2(t_1)}{2A'(\theta)} \quad (20)$$

where En_2 is the potential energy accumulated in the ground in the second phase.

4.3 Sticking-restitution Phase $[t_2, t_3]$

The rod is still sticking on the ground during this phase, namely $|F_t| \leq \mu F_n$. On the assumption that the definition of Stronge's coefficient is valid, the restitution potential energy released in this phase can be written by

$$En_r = -e_s^2 En_c = -e_s^2 (En_1 + En_2)$$

Here En_r is negative, which represents the potential energy released. And hence

$$\begin{aligned} \dot{x}_A(t_3) &= 0 \\ \dot{y}_A(t_3) &= \sqrt{-2A'(\theta)En_r} \\ \dot{\theta}(t_3) &= \dot{\theta}(t_2) - \frac{3 \cos \theta}{4l} \dot{y}_A(t_3) \end{aligned} \quad (21)$$

When the rod is in the inconsistent state, we can get the velocity jump after impact using (14), (18) and (21).

Because the jump rule is deduced on the basis of the approximate impulse theory, it is valid only when the system rigidity is big enough. In this paper, elastic modulus of Painlevé's example should be more than 10^{14} N/m^2 if the results of the theoretical jump rule is precise enough.

5 CONCLUSION

Numerical research is carried out on the dynamic motion of Painlevé's example by using a bi-nonlinear impact model in the normal direction and Coulomb's friction law in the tangential direction. The numerical research solves Painlevé's paradox. A jump rule of "IW/OC" is derived in this paper from an approximate impulse theory and the coefficient of restitution

defined by Stronge. The results of the jump rule are quite precise if the system rigidity is big enough.

REFERENCES

- 1 Pfeiffer F, Glocker CH. Unilateral Multibody Contact. Netherlands: Kluwer Academic Publishers, 1998
- 2 Pfeiffer F, Glocker CH. Multibody Dynamics with Unilateral Contacts. New York: Wiley and Sons, 1999
- 3 Brogliato B. Nonsmooth Mechanics, Models, Dynamics and Control. London: Springer-Verlag London Limited, 1999
- 4 Tzitzouris JA. Numerical resolution of frictional multi-rigid-body system via fully implicit time-stepping and nonlinear complementarity. [Ph D Thesis]. Baltimore, Maryland: Hopkins University, 2001
- 5 Wang Y, Mason MT. Two-dimensional rigid-body collisions with friction, *ASME J Appl Mech*, 1992, 59: 635~642
- 6 Song P, Kraus P, Kumar V, Dupont P. Analysis of rigid-body dynamic models for simulation of systems with frictional contacts. *ASME J Appl Mech*, 2001, 68: 118~128
- 7 Chen B, Yan ZX, Zhao Z. The impact model resolution of Kane dynamic puzzle. *Acta Mechanica Sinica*, 2002, 34 (Supplement): 43~47 (in Chinese)
- 8 Johnson KL. Contact Mechanics. New York: Cambridge University Press, 1985
- 9 Vu-Quoc L, Zhang X, Lesburg L. A normal force-displacement model for contacting spheres accounting for plastic deformation: force-driven formulation. *ASME J Appl Mech*, 2000, 67: 363~371
- 10 Liu CS, Chen B. A normal force-displacement model for impacting rigid body accounting for elastic-plastic deformation. *Acta Mechanica Sinica*, 2002, 34 (Supplement): 57~60 (in Chinese)
- 11 Shivaswamy S. Modeling contact forces and energy dissipation during impact in mechanical systems. [Ph D Thesis]. Ann Arbor MI: UMI, 2002
- 12 Poston T, Stewart I. Catastrophe Theory and Its Applications. London: Pitman Publishing Limited, 1978